Article:
Zhang, Z, Gao, Y, Meldrum, FC orcid.org/0000-0001-9243-8517 et al. (4 more authors) (2020) Investigating the Nucleation Kinetics of Calcium Carbonate Using a Zero-Water-Loss Microfluidic Chip. Crystal Growth & Design, 20 (4). pp. 2787-2795. ISSN 1528-7483

https://doi.org/10.1021/acs.cgd.0c00191

Investigating the Nucleation Kinetics of Calcium Carbonate Using a Zero-Water-Loss Microfluidic Chip

Zongwei Zhang [a,†], Yuan Gao [a,†], Fiona C. Meldrum [b,], Lingling Shui [c], Zhijun Wang [d], Shunbo Li [a,*] and Gang Li [a,*]*

a. Key Laboratory of Optoelectronic Technology and Systems, Ministry of Education & Key Disciplines Laboratory of Novel Micro-Nano Devices and System Technology, College of Optoelectronics Engineering, Chongqing University, Chongqing, China
b. School of Chemistry, University of Leeds, Leeds, LS2 9JT, UK.
c. Guangdong Provincial Key Laboratory of Optical Information Materials and Technology, South China Normal University, Guangzhou 510006, China
d. State Key Laboratory of Solidification Processing, Northwestern Polytechnical University, Xi'an 710072, People's Republic of China

† These authors contributed equally to this work

* Corresponding Authors:

Shunbo Li (shunbo.li@cqu.edu.cn), Gang Li (gang_li@cqu.edu.cn) and Fiona C. Meldrum (F.Meldrum@leeds.ac.uk)

KEYWORDS: nucleation rate; calcium carbonate; microfluidic chip; zero-water-loss; surfactant-free

ABSTRACT

Characterization of nucleation processes is essential to the development of strategies to control crystallization in many industrial, atmospheric, biological, and geological environments. An effective route to studying nucleation processes is the use of large numbers of small, identical volumes, where these minimize the effects of impurities that can dominate in bulk solution and allow the stochastic nature of nucleation to be considered. Here, we present a multilayered microfluidic device for nucleation studies that can be used to carry out 10 000 simultaneous reactions in identical microcavities, and 500 of them are used for investigating nucleation kinetics. Unlike droplet-based systems, no surfactants are required, and the presence of an integrated water

reservoir prevents water loss, allowing studies to be performed for long durations. This device was used to study the nucleation of calcium carbonate in the presence and absence of magnesium ions. Two distinct nucleation rates of 286 $cm^{-3}s^{-1}$and 12.6 $cm^{-3}s^{-1}$were observed in the absence of magnesium, where the rapid rate likely derives from microcavities containing impurities. The nucleation rate was then significantly reduced in the presence of magnesium ions, and the profile was more complex. This device is therefore an ideal platform for studying slow nucleation processes in surfactant-free environments.

1. INTRODUCTION

Precipitation of calcium carbonate (CaCO3) is of great significance to many fields including biomineralization, geology, carbon sequestration, and in industrial applications such as paper coatings and fillers. [1,2] Understanding the mechanisms underlying the nucleation and growth of calcium carbonate is therefore of considerable importance, where this offers the potential to control multiple features including polymorph, size, and morphology. Investigation of nucleation processes remains particularly challenging as they are strongly influenced by the presence of impurities and surfaces, and measurements are ideally carried out under conditions of constant supersaturation.[3,4]

The most straightforward method of studying nucleation is by separating them into large numbers of droplets or vessels. These facilitate statistical analysis, and when the number of droplets greatly exceeds the number of impurities present in the initial volume, the majority of droplets will be theoretically impurity-free. Emulsions or droplets generated by ultrasonication, magnetic stirring, or jet homogenizer have been widely applied to study the nucleation kinetics of organic compounds such as hexadecane and cocoa butter.[5-7] However, the polydispersity of droplets would greatly influence the investigation of nucleation kinetics. To overcome these drawbacks, microfluidic technology is then developed as a convenient route for generating large numbers of

identical droplets whose volumes can be finely tuned. Sample solutions could be discretized into droplets with sizes in the range between a few micrometers to hundreds of micrometers by another immiscible phase in typical microfluidic chips with T-junction or flow focusing junctions. These droplets are considered as independent microvessels for crystallization studies. Thermal control as a means to induce crystallization can be easily implemented on-chip, and analytical tools such as optical microscopy and X-ray scattering (or diffraction) can be used to monitor crystallization process within the droplets.[8,9] The microfluidic technologies are therefore growing in popularity as a means of studying nucleation kinetics.[10-12]

Most of these reported studies focus on investigating highly soluble compounds such as proteins and KNO_3, where nucleation is readily induced by evaporation of water or change of temperature. Far fewer have studied poorly soluble compounds, where nucleation typically occurs from a metastable solution under isothermal conditions. There are a number of technical challenges associated with these measurements, however. Device fouling can readily occur when reaction solutions are combined to form droplets,[13] and measurements are often conducted over long times.[14] The droplets must therefore be kept isolated to prevent merging, the evaporation of water can occur and result in supersaturation changes, and the addition of surfactants to stabilize droplets can influence nucleation.[13,15] In order to avoid the interference from surfactants, different means have been developed to prevent droplet merging in a surfactant-free system. A long tubing is employed to avoid coalescence for protein crystallization with a long incubation time.[16,17] However, the throughput is not satisfied; a length of 2 m has to be used to store 200 droplets. Physical isolation using wells[18] rather than moving droplets is an alternative way, and the throughput could be much higher. To reduce water-loss in droplets, lots of techniques have been reported, such as putting the whole chip under water,[19] Parylene coating in the PDMS chip,[20] use

of glass for chip fabrication,[21] storing droplets in glass capillary[22] or PTFE tubing,[23] etc. However, they encountered different problems; for instance, putting the whole device in a water bath hindered real-time observation of crystallization, the fabrication process of glass microfluidic chip is not as simple as PDMS chip, and the use of capillary or tubing for droplets storage is difficult for ultrahigh throughput crystallization studies in droplets. Here, we present a microfluidic device for conducting in situ nucleation studies that can offer long-term storage of up to 10 000 isolated, surfactant-free droplets.

This is achieved using a glass-PDMS-glass sandwich construction and integrated water reservoir that prevents water loss. Our new device therefore facilitates long-term studies of nucleation at constant supersaturation and temperature, where the huge number of droplets facilitates statistical analysis. We then demonstrate its application to study the nucleation of calcium carbonate under low supersaturation conditions. The effect of inorganic additive Mg in the nucleation kinetics will also be investigated.

2. EXPERIMENTAL SECTION

2.1. Microfluidic Chip Design and Fabrication.

Figure 1 shows a schematic diagram of the high-throughput, zero-water-loss microfluidic chip employed here. The chip consists of six layers (Figure 1a): two PDMS oil reservoirs at the inlet and outlet to supply the oil phase, the top and bottom glass substrates as vapor barriers, a thin PDMS film under the top glass substrate to avoid the impurity and surface defects from the top glass slide, a micropatterned PDMS film as the microcrystallizer, and a PDMS chamber (shown as cavity PDMS) under the microcrystallizers which is filled with the water reservoir. Each PDMS layer is of a similar size to the supporting glass slide (25 mm × 75 mm), such that they are readily

fabricated on the glass slide and viewed using an optical microscope. The master for the PDMS water-reservoir is fabricated by laser cutting on a PMMA plate such that it has an external frame wall of size 2 mm (height) × 25 mm (width) × 75 mm (length) and an internal frame wall size of 2 mm (height) × 21 mm (width) × 71 mm (length). In accordance with our previous design,[24,25] each device contains 10 000 cylindrical microcavities for holding the partitioned droplets, where these are connected by microchannels which allow transport of solutions. These features have the following dimensions: microchannel is 46 μm (height) × 80 μm (width), microcavity is 110 μm (height) × 100 μm (diameter), and the volume of the crystallization microcavity is calculated to be 0.86 nL. Microfluidic devices were fabricated from PDMS using soft lithography and laser cutting. The masters for the patterned microcavities and the water reservoir were fabricated on silicon wafers and poly (methyl methacrylate) (PMMA) plates, respectively. The PDMS prepolymer and curing agents were mixed in a 10:1 weight ratio, degassed, and poured over the two masters. A poly (ethylene terephthalate) (PET) film was then placed over each mixture, and a glass plate of mass 5 g was placed on the top. The PET film provided an easy way to peel off the fragile molded PDMS film from the masters after curing. All of the sandwiched PDMS mixtures were cured in an oven for 1.5 h at 80 °C. After detachment from the master, the PET/PDMS micropatterned film was aligned with, and bonded to the top glass slide after plasma treatment. Prepunched holes provided solution inlets and outlets. The PET/PDMS waterreservoir film was then aligned and bonded to the bottom glass side using plasma bonding, with predrilled holes providing water inlets and outlets. Finally, the PDMS oil reservoirs were bonded to the glass slide after plasma treatment.

2.2. Chemicals and Solution Preparation.

SU-8 was purchased from MicroChem (Newton, MA, USA), and PDMS (Sylgard 184 kit) was provided by Dow Corning (Midland, MI, USA). $CaCl_2$, Na_2CO_3, $MgCl_2$ and paraffin oil were

purchased from Chron Chemicals (Chengdu, China). 20 mM $CaCl_2$, 20 mM Na_2CO_3, and 80 mM $MgCl_2$ stock solutions were prepared in deionized water and were diluted to give (1) a solution of concentration $[CaCl_2] = [Na_2CO_3] = 3$ mM for studying the nucleation kinetics of calcium carbonate, and (2) solutions of concentrations $[CaCl_2] = [Na_2CO_3] = 3$ mM, 2.5 mM, 2 mM $CaCl_2$/ $MgCl_2$ ratios of 1:4, for studying additive effects.

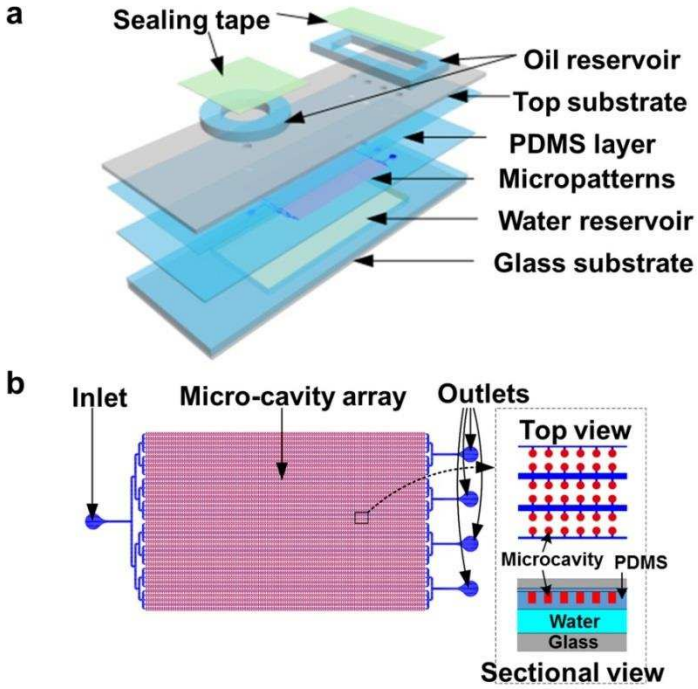

Figure 1. Schematic diagram of the zero-water-loss high-throughput microfluidic chip. (a) 3D view; (b) Microcavity array for crystallization, the top view and the sectional view of the device.

2.3. Chip Operations.

A schematic diagram of the operation of the microfluidic chip is shown in Figure 2. The crystallization solution was loaded into the microfluidic device by vacuum degassing, where the chip was placed in a Petri dish containing freshly prepared solution, and degassing was performed for 1.5 min. No crystallization occurred during this time; however, the solution was under a metastable state due to the premixing before loading. The chip was then removed from the vacuum, and the water reservoir in the chip was filled with deionized (DI) water using a syringe. Finally,

the microchannels were filled with paraffin oil using a suction pen in order to isolate the individual microcavities. All of the inlet and outlet reservoirs of the chip were filled with paraffin oil, and the chip was placed on a microscope stage. The total time for solution loading into the microfluidic chip was about 3 min, indicating the present system was suitable for long-term crystallization study and could not be employed for fast nucleation experiment.

2.4. Crystallization in Bulk Solution.

Calcium carbonate was also precipitated in bulk solution in order to compare the nucleation rate and products with those generated on-chip. A bulk reactor with diameter of 1 mm was made using PDMS such that the material environment was identical to that in the microfluidic chip. The calcium carbonate solution was placed in the reactor, and crystallization was monitored using optical microscopy.

2.5. Material Characterizations.

The precipitation of $CaCO_3$ crystals within the microfluidic chip was observed using an optical microscope fitted with cross-polarizers (NMM-800RFTRF, Novel Optic, Ningbo, China). A total of 500 droplets were used to observe the nucleation events, and the time for the observation was about 5 min for one round. Scanning electron microscope (SEM) images of $CaCO_3$ crystals were taken using a ZEISS Auriga SEM/FIB Crossbeam system (ZEISS, Germany) operating at 5 kV. Identification of crystal polymorph was carried out using a Raman microscope (LabRAM HR Evolution, HORIBA Jobin Yvon S.A, France) equipped with a 532 nm laser. The data were further analyzed using OriginPro 8 software (OriginLab, Northampton, MA) and Matlab (MathWorks, Natick, MA).

2.6. Analysis of Nucleation Kinetics.

Because of the excellent optical transmittance of PDMS and glass, the nucleation process could be directly studied using an optical microscope fitted with crosspolarizers. Crystals within individual droplets were identified as bright spots under cross-polarized illumination due to their birefringence. Approximately 500 droplets were studied in each experiment, and the cumulative probability P(t)[26] that no nuclei are formed within t could be calculated using the following equation and plotted as a function of time.

$$\mathrm{P(t)} = \frac{\mathrm{N_0(t)}}{\mathrm{N}} \qquad (1)$$

where $N_0(t)$ is the number of droplets without any crystal at a given time t, and N is the total number of droplets. If the nucleation events occur continuously and independently with a constant nucleation rate J, the cumulative probability is given by a simple exponential equation (eq 2).

$$\mathrm{P(t)} = e^{-JVt} \qquad (2)$$

where J ($cm^{-3}s^{-1}$) is the volume nucleation rate (usually called nucleation rate for simplicity) representing the nucleation rate per unit volume, and V (cm^3) is the volume of droplets. Consequently, a plot of $ln(P(t))$ versus t should result in a straight line. If the system does not have a constant nucleation rate, the plot of $ln(P(t))$ versus t would show a strong nonlinearity. Therefore, the plot of $ln(P(t))$ versus t is also conducted in our analysis of nucleation kinetics.

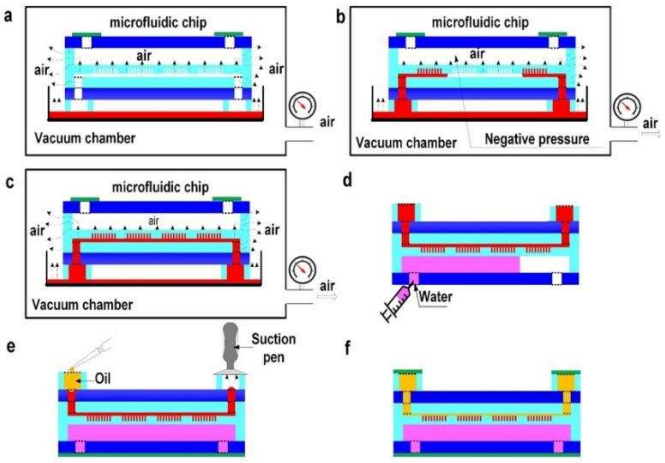

Figure 2. Schematic diagram of the operation of the chip to study calcium carbonate nucleation: (a-c) solution loading by vacuum degassing; (d) water loading into the water reservoir; (e) oil loading to isolate the microcavities; (f) inlet and outlet were closed using PDMS.

3. RESULTS

3.1. Water Loss in the Microfluidic Chip.

The gas permeability nature of PDMS could lead to water evaporation during microfluidic experiments, especially under the elevated temperature or long running period.[24] The sorption of water into PDMS is another factor one has to consider in small volume reactors for concentration sensitive reactions. In our experiments, a channel outgas technique[27] was used for solution loading. This process not only drove out the gas trapped in the channels and wells of PDMS chip, but also evacuated the gas dissolved in the bulk PDMS. When the degassed PDMS chip was brought back into the atmosphere, air molecules in the surrounding space and water molecules in the channel were absorbed into PDMS bulk of the chip to establish a new pressure equilibrium, leading to saturation of PDMS with water vapor. Thus, the degassing-based solution loading process is helpful to saturate PDMS with water before experiment. The ability of the designed microfluidic chip to prevent water loss was demonstrated by comparing water loss from chips with three configurations: a PDMS chip, a glass- PDMS-glass (G-P-G) sandwiched chip and a G-P-G chip combined with a water reservoir. Figure 3 shows the water loss from droplets in these three configurations over 96 h (4 days).

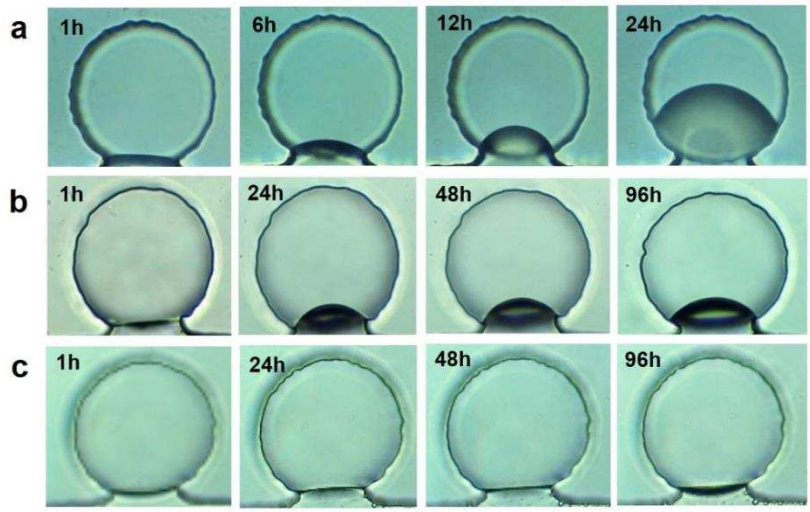

Figure 3. Comparison of the water loss in the microfluidic chips assembled with three different configurations at room temperature: (a) PDMS chip; (b) Glass-PDMS-glass sandwich chip; (c) glass-PDMS film-glass sandwich chip integrated with a water supplement chamber.

A total loss of about 0.33 nL, which is equivalent to over 35% of the total volume, occurred from droplets in the PDMS chip over just 24 h. The water loss for the G-P-G chip was about 0.052 nL (6% of the total volume) after 4 days. In contrast, no water loss was observed after 4 days for droplets trapped within the G-P-G chips integrated with a water reservoir. The latter device is therefore ideally suited for studying nucleation over a long time

3.2. Nucleation of Calcium Carbonate under Additive-Free Conditions.

To investigate nucleation kinetics of calcium carbonate, the microcavity arrays in the microfluidic chip were filled with supersaturated calcium carbonate solution of concentration $[Ca^{2+}] = [CO_3^{2-}] = 3$ mM using the method described in the Chip Operation section.The nucleation events in ~500 droplets were monitored and recorded over 24h using polarized light microscopy. Three experiments were performed for each condition, and the mean values and standard deviations were calculated. The percentage of droplets which did not contain crystals (the

cumulative probability P(t)) was plotted versus time in Figure 4a, and a plot of $ln(P(t))$ versus t is shown in Figure 4b. P(t) decreases very rapidly in the first 6h and then very gradually decreases with longer incubation times. That there is not a simple straight-line relationship between $ln(P(t))$ and t also demonstrates that a number of nucleation mechanisms operate. The findings are quite similar to the reported results when studying nucleation of various materials.[28-31] The nonlinear curve in Figure 4b indicates that the nucleation is not first order and the existence of heterogeneous nucleation is a plausible interpretation due to the presence of impurities. The cumulative probability was therefore fitted to a two-exponential model to extract individual nucleation rates:[27,32]

$$P(t) = ae^{-k1t} + (1-a)e^{-k2t} \qquad (3)$$

where a is the coefficient, and k1 and k2 are the droplet nucleation rates corresponding to the individual droplets in the designed microfluidic chip showing different nucleation mechanisms. Equation 3 was used to fit the data shown in Figure 4a, where the plot is shown in red. The explicit form of fitting curve was shown in eq 4:

$$P(t) = 0.87e^{-0.885t} + 0.13e^{-0.039t} \qquad (4)$$

Nucleation mechanism 1 has a larger coefficient (0.87) and faster nucleation rate $k1 = 0.885\ h^{-1}$ and therefore dominates the process. The volume nucleation rates were also be calculated $J1 = k1/V_{drop} = 286\ cm^{-3}s^{-1}$ and $J2 = k2/V_{drop} = 12.6\ cm^{-3}s^{-1}$. Nucleation rate 2 was therefore about 20 times in magnitude smaller than nucleation rate 1. Nucleation 1 is therefore attributed to heterogeneous nucleation on impurities within the droplets, while Nucleation 2 is either homogeneous or slow heterogeneous nucleation associated with the chamber walls. The precipitated crystals after 24h are all calcite confirmed by Raman spectroscopy (Supplementary Figure S1).

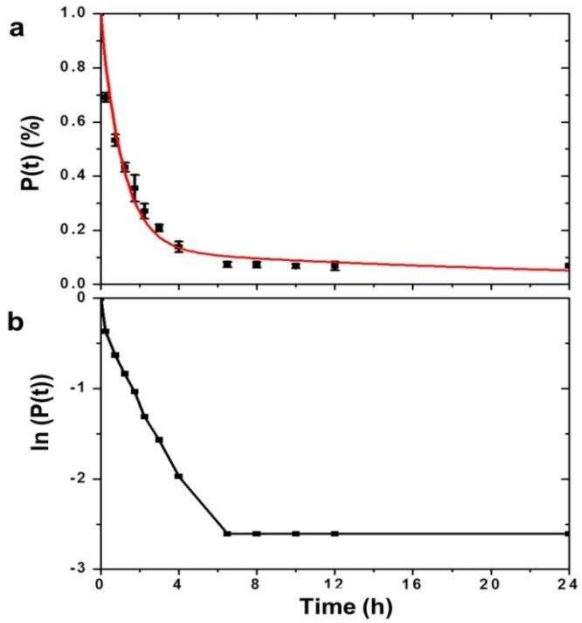

Figure 4. evolution of the cumulative probability P(t) (a) and $ln(P(t))$ (b) in 24h (black squares) during $CaCO_3$ nucleation without magnesium in the designed microfluidic chip. The red line is the fitted curve. The final concentrations of [Ca^{2+}] and [CO_3^{2-}] are 3 mM.

3.3. Nucleation of Calcium Carbonate with Addition of Magnesium.

The microfluidic device was also used to investigate the influence of magnesium ions on the nucleation of calcium carbonate. Magnesium is abundant in the environment and has significant effects on calcium carbonate precipitation, stabilizing amorphous calcium carbonate (ACC),[33] changing crystal morphologies, substituting for Ca^{2+} in the calcite lattice, and promoting aragonite formation.[34-36] Nucleation studies were again conducted by creating arrays of droplets of supersaturated calcium carbonate solution in the microfluidic devices. Solutions where prepared by combining $CaCl_2$, $MgCl_2$ and Na_2CO_3 solutions to give compositions of [Ca^{2+}] = [CO_3^{2-}] = 3 mM, 2.5 mM, or 2 mM with [Ca^{2+}]/ [Mg^{2+}] =1:4. Three experiments were performed at each condition to demonstrate reproducibility.

Figure 5a shows the change in P(t) with respect to time at the different supersaturations, while Figure 5b shows a plot of $ln(P(t))$ versus time. The nucleation process of calcium carbonate without magnesium is also shown here for comparison. As clearly demonstrated, addition of magnesium retarded nucleation, where induction times of ~ 0.5 h were recorded for all of the reaction conditions. The curves all exhibited similar shapes, and nucleation rates were higher at higher supersaturations. The nucleation process could be divided into three regions: (1) slow heterogeneous nucleation (0-7h); (2) fast heterogeneous nucleation (7-12 h); and (3) homogeneous nucleation (>12 h) (or with minor contribution from the environment). However, the evolution of P(t) could not be fitted with simple combinations of exponentials. The duration of heterogeneous nucleation was extended from 6h (without magnesium) to 12h (with magnesium), confirming that magnesium inhibits calcite formation, which in turn stabilizes ACC.[37]

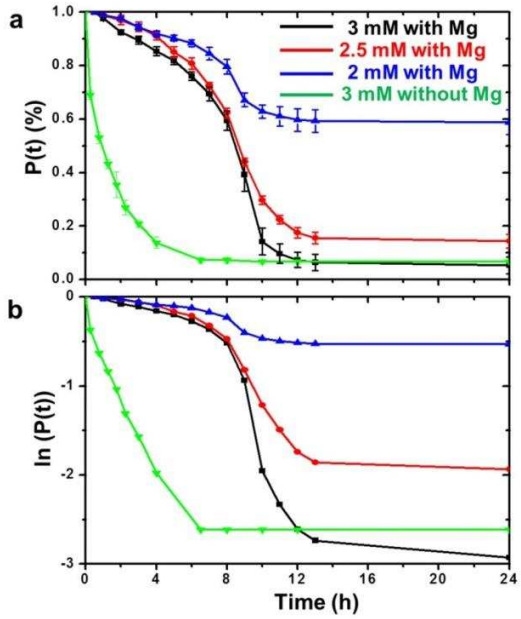

Figure 5. evolution of the cumulative probability P(t) (a) and ln(P(t)) (b) in 24 h during $CaCO_3$ nucleation with magnesium and without magnesium in the designed microfluidic chip. Initial concentrations of $[Ca^{2+}] = [CO_3^{2-}]$ = 3 mM, 2.5 mM ,and 2 mM with magnesium ($[Ca^{2+}]/[Mg^{2+}]$ =

1:4) are shown in black, red, and blue respectively ,and initial concentrations of $[Ca^{2+}] = [CO_3^{2-}] = 3$ mM without magnesium is shown in green.

The crystals generated in the presence of magnesium were also characterized using optical microscopy, scanning electron microscopy (SEM) (Figure 6), and Raman microscopy (Figure 7). The vast majority of droplets only contained a single crystal, where SEM showed that most exhibited lens-like or wheatsheaf morphologies that are characteristic of aragonite. The crystal growth process after nucleation (Supplementary Figure S2) was followed using optical microscope under higher magnification. Figure S2 showed the growth could be finished in less than 1h, and the crystal morphology could be roughly identified to be rod shape. No phase transformation was observed from nucleation to the final product. The presence of peaks at 1086, 701, and 206 cm^{-1} in the Raman spectra confirmed that the crystals were aragonite,[38] where the additional peaks in the spectrum correspond to the PDMS.

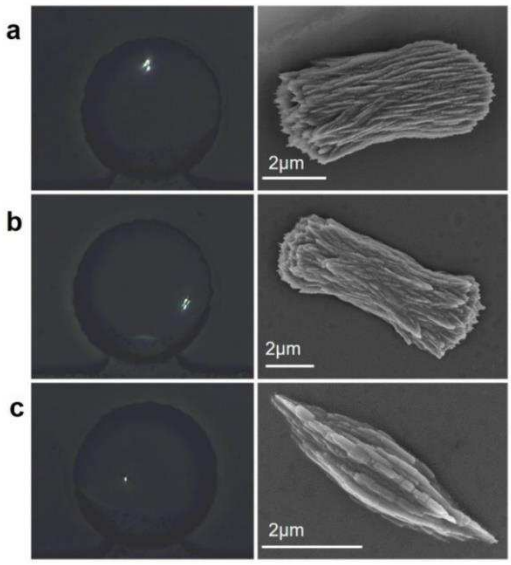

Figure 6. Optical micrographs with cross-polarizer and SEM images of aragonite crystals formed in the microdroplets under different calcium concentration with magnesium ($[Ca^{2+}]/[Mg^{2+}]$ = 1:4): (a) 3 mM, (b) 2.5 mM and (c) 2 mM.

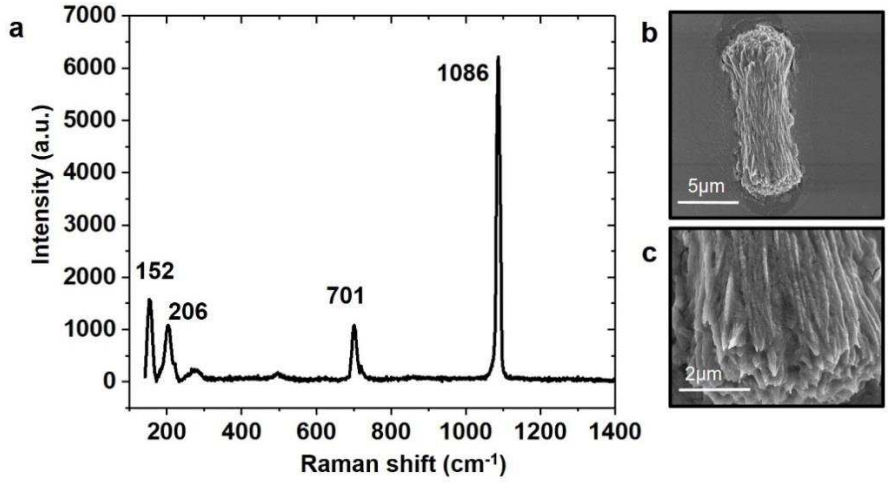

Figure 7. Raman spectrum (a) and the corresponding SEM images of aragonite crystals (b, c) formed in microfluidic devices with calcium concentration of 3 mM with magnesium ($[Ca^{2+}]/[Mg^{2+}]$ = 1:4).

3.4. Comparison between Nucleation in Bulk Solution and in the Microfluidic Chips.

In order to compare crystallization in the isolated microdroplets and in bulk, calcium carbonate was also precipitated from 150 μL volumes in wells prepared in PDMS. Figure 8 showed the crystallization process taken by an optical microscope in the bulk experiment. In additive-free solutions, calcium carbonate crystals started to form in around 5 min, and crystallization terminated in 20 min in bulk (Figure 8a) as compared with 6h in the chambers in the microfluidic devices. When magnesium was also present, nucleation in bulk occurred in a burst at ~15 min at all supersaturations, where more particles formed at higher supersaturations (Figure 8b-d). The crystals then continued to grow in size, and crystallization terminated in ~1 h in bulk solution as

compared with over 12 h in the microdroplets. All of the crystals observed were calcite without magnesium and aragonite with magnesium ($[Ca^{2+}]/[Mg^{2+}]$ =1:4), as demonstrated using Raman microscopy, and they possessed morphologies that were also comparable to those formed in the microfluidic device. However, they were larger in size (10-20 μm in bulk as compared with 3-8 μm in droplets), which demonstrates that growth in the droplets was limited by the available reactants.[39] These experiments therefore demonstrate the dramatic difference in nucleation in bulk as compared with small volumes, where unavoidable impurities and surfaces dominate in bulk.

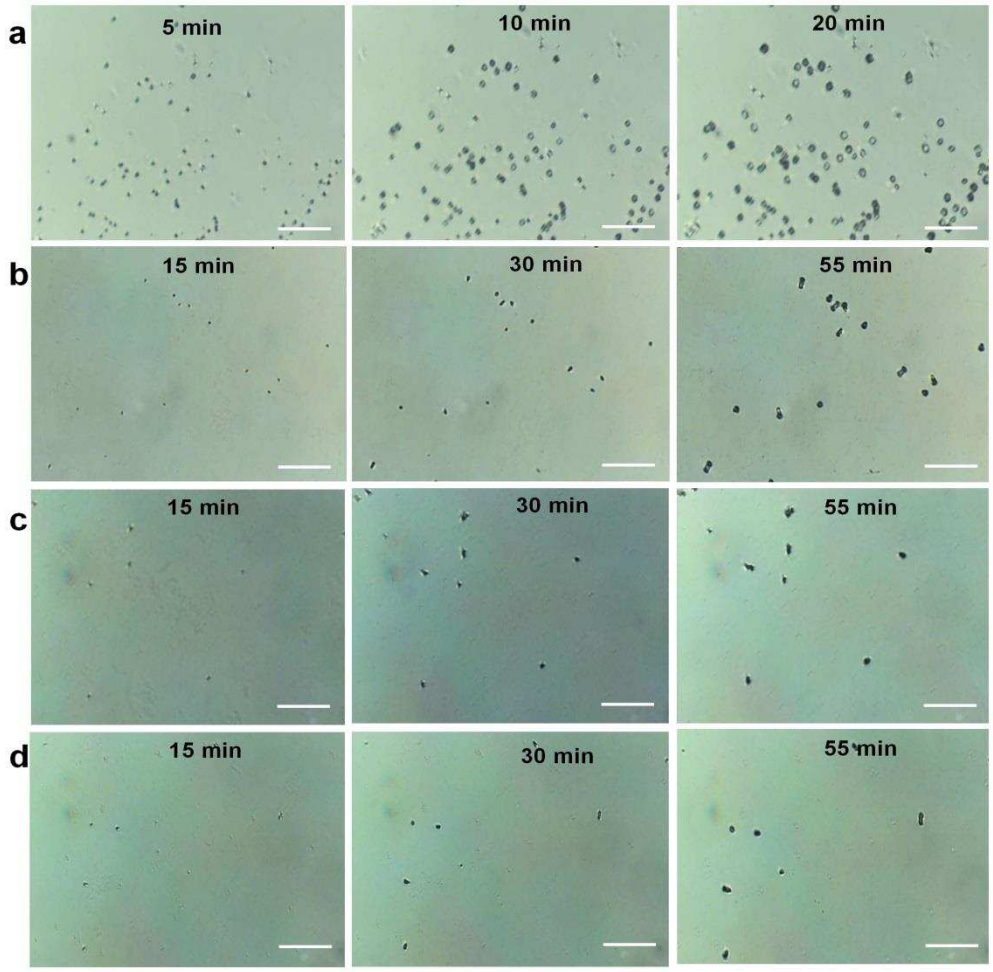

Figure 8. Calcium carbonate crystals formed in bulk solution at the times indicated from (a) 3mM $CaCl_2$ and Na_2CO_3, (b) 3mM $CaCl_2$, 3mM Na_2CO_3 , and 12 mM $MgCl_2$, (c) 2.5mM $CaCl_2$, 2.5mM

Na_2CO_3 and 10 mM $MgCl_2$, (d) 2mM $CaCl_2$, 2mM Na_2CO_3 , and 8 mM $MgCl_2$. The scale bars were 50 µm.

4. DISCUSSION

The microfluidic device described here presents a huge number of reaction chambers that offer defined microenvironments and which support high-throughput analysis. Incorporating a reservoir that prevents evaporation, they also facilitate long-duration experiments. Nucleation in bulk solution is affected by factors including the presence of impurities and the walls of the reaction vessel, and it can be difficult to probe the stochastic nature of nucleation.[40,41]Large numbers of isolated, small scale systems are therefore desired.[42]The highthroughput microfluidic platform presented here achieves this goal by partition by presenting a large number of small reaction chambers. Each is of identical size (~0.86 nL), droplet coalescence is avoided, and the system is surfactant-free. As also demonstrated, because of the permeability of PDMS to water vapor, evaporation from aqueous droplets can be a serious problem in microfluidic chips. This is particularly important in crystallization studies that can run for several days, and where the droplet size must be invariant in order to preserve the supersaturation. A range of approaches have been explored to reduce such water-loss such as placing the whole chip under water, coating chips with parylene using vapor deposition techniques, and enclosing devices in glass or polymer.[43,44] The device described here uses two means to prevent water loss. First, sandwiching the PDMS between two glass slides prevents most water loss from the top and the bottom of the chip. In order to prevent water loss from the sides-where this becomes important in long runs of several days-a water-filled chamber is also integrated into the chip. The high permeability of PDMS to water vapor enables the continuous diffusion of water molecules from the water reservoir into the

droplets through the thin PDMS membrane, which compensates for any loss by evaporation. The droplet size and supersaturation therefore remain constant (Figure 3).

This microfluidic chip design was used to study the nucleation of calcium carbonate under additive-free conditions and in the presence of magnesium ions. The use of droplets allows us to distinguish between droplets containing impurities, and those that are impurity-free, while the ability to maintain constant volumes over long time periods is essential for obtaining accurate nucleation rate data. Considering other factors that influence the accuracy of the data, induction times were estimated using polarized optical microscopy. While crystals can only be detected once they have achieved micrometer sizes, the discrepancy between the measured and "true" nucleation time is small as the time taken for the crystals to grow is short compared with the induction time. The discrepancy is the time for crystals to grow from nanometer size to micrometer size. According to the experimental observations, the growth times of crystals from detectable size to the end size of final products are similar between droplets and bulk solutions. As a rough estimation, the discrepancies are about 5 min without additive and 15 min with magnesium ($[Ca^{2+}]/[Mg^{2+}] = 1:4$), which are demonstrated by the first column in Figure 8. On the contrary, the induction time for the whole chip is longer than 6h even for the fast nucleation rate as shown in Figure 5. Therefore, the discrepancy between the measured and "true" nucleation time could be neglected. In addition, the crystal habit could also be roughly distinguished when using high magnification of the optical microscope (Figure S2). The experiments conducted here also used only 500 of the 10 000 available reaction chambers due to the time taken to visualize the crystals in these microcavities in the current setup. The total period of about 5 min is taken for visualization of crystals during moving the microscope stage, which is negligible compared to the whole nucleation process (hours). Thus, the observation of 500 droplets is assumed to be simultaneous. With the

implementation of an automated stage and image-processing software, it would be straightforward to employ all of these reaction environments in a single data set.

Looking then at the data obtained on calcium carbonate nucleation, a huge difference in induction times can be seen between the droplets and bulk solution. Nucleation in the additive-free system could be fitted to a double exponential function, where the rapid (heterogeneous) nucleation rate was about 20 times of magnitude greater than the slower (homogeneous) nucleation rate (Figure 4). It is noted, however, that the slow rate is unlikely to correspond to true homogeneous nucleation, where the chamber walls may offer a small advantage for nucleation.[45] Almost 90% of droplets belonged to the rapid nucleation regime. Given that all of the droplets are of the same size and occupy the same environments, this provides strong evidence that impurities are present in most (but not all) droplets, which promote nucleation.

The nucleation rates in the additive-free system can also be compared with that determined for the crystallization kinetics of amorphous calcium carbonate (ACC) within 100 μm diameter surfactant-stabilized droplets held in individual wells.[14] ACC precipitation occurred within 30 min on exposure of droplets of 1 M calcium chloride solution to ammonium carbonate vapor, and its subsequent transformation to crystalline phases was monitored over the following 5 days. A nucleation rate of 1.2 cm^{-3} s^{-1} was determined, and once a calcite particle was detected, it grew within 1 h to consume all of the ACC.

The solution composition of $[CaCl_2] = [Na_2CO_3] = 3$ mM exceeds the solubility of ACC, but little ACC is precipitated at this supersaturation.[46] In our tudies, the rapid nucleation rate is 286 cm^{-3} s^{-1}, and slower nucleation rate is 12.6 cm^{-3} s^{-1}. The latter is 10 times larger than that with an upper limit of 1.2 cm^{-3} s^{-1} reported for the transformation of ACC to vaterite and calcite.[14] The

latter study was conducted by exposing microfluidic droplets containing 1 M $CaCl_2$ solution to ammonium carbonate vapor, where extensive precipitation of ACC occurred. The solution compositions prior to nucleation will therefore not be identical in both experiments. Moreover, surfactant was added in the reported work, and the present one is surfactant-free, which is possibly the factor for the nucleation retardation. Nucleation was then significantly suppressed by the addition of magnesium ions, as is widely recognized.[33,37,47] The nucleation kinetics could be divided into three regimes (Figure 5), but could not be adequately described by a function comprising a small number of exponentials. The unusual nucleation curves from the crystallization with magnesium come from the inhibition effect of magnesium and suggest different nucleation pathways[48,49] in the system, which is also evidenced by different crystal morphologies shown in Figure 6. The existence of a number of nucleation mechanisms is also consistent with other findings when studying the nucleation of other crystals in small volumes. [29,30,50]

5. CONCLUSIONS AND PERSPECTIVES

This paper presents a high-throughput and zero-water-loss microfluidic chip with 10 000 microcavities (droplets), where a multilayer structure and integral water chamber beneath the microcavities were key to preventing water evaporation. It was then employed to study the nucleation kinetics of calcium carbonate in the absence and presence of magnesium ions, where maintenance of a constant volume is essential for studying slow nucleation processes. All of 500 droplets were used to visualize the crystals in the current setup. Our results showed that nucleation was significantly slower in these microcavities as compared with bulk solution and that nucleation in the additive-free solutions could be described by a double exponential function. This was attributed to heterogeneous nucleation in droplets containing impurities, where nucleation that was about 20 times in magnitude slower in impurity-free droplets. The addition of magnesium then

significantly retarded nucleation. This microfluidic device therefore presents an excellent platform for performing longterm nucleation studies in aqueous solutions, with the additional advantages of low contamination levels, surfactantfree conditions, good stability, and the opportunity for highthroughput measurements. Further improvements such as image capture and analysis, and the use of a clean room environment to minimize the introduction of impurities could be developed in the future.

ASSOCIATED CONTENT

Supporting Information

The Supporting Information is available free of charge at https://pubs.acs.org/doi/10.1021/acs.cgd.0c00191.

The Raman spectrum of calcite and optical images of the crystal growth in microdroplets.

AUTHOR INFORMATION

Corresponding Authors

* **Shunbo Li** - Key Laboratory of Optoelectronic Technology and Systems, Ministry of Education & Key Disciplines Laboratory of Novel Micro-Nano Devices and System Technology, College of Optoelectronics Engineering, Chongqing University, Chongqing, China;

Email: shunbo.li@cqu.edu.cn

* **Gang Li** - Key Laboratory of Optoelectronic Technology and Systems, Ministry of Education & Key Disciplines Laboratory of Novel Micro-Nano Devices and System Technology, College of Optoelectronics Engineering, Chongqing University, Chongqing, China;

Email: gang_li@cqu.edu.cn

* **Fiona C. Meldrum** - School of Chemistry, University of Leeds, Leeds, LS2 9JT, UK;

Email: F.Meldrum@leeds.ac.uk

Other Authors

Zongwei Zhang - Key Laboratory of Optoelectronic Technology and Systems, Ministry of Education & Key Disciplines Laboratory of Novel Micro-Nano Devices and System Technology, College of Optoelectronics Engineering, Chongqing University, Chongqing, China

Yuan Gao - Key Laboratory of Optoelectronic Technology and Systems, Ministry of Education & Key Disciplines Laboratory of Novel Micro-Nano Devices and System Technology, College of Optoelectronics Engineering, Chongqing University, Chongqing, China

Lingling Shui - Guangdong Provincial Key Laboratory of Optical Information Materials and Technology, South China Normal University, Guangzhou 510006, China orcid.org/ 0000-0001-8517-1535

Zhijun Wang - State Key Laboratory of Solidification Processing, Northwestern Polytechnical University, Xi'an 710072, People's Republic of China

Complete contact information is available at:

https://pubs.acs.org/10.1021/acs.cgd.0c00191

Author Contributions

#Z.Z. and Y.G. contributed equally to this work. S.L. and G.L. designed the experiments. Z.Z. and G.Y. did the experiments, collected data, and wrote the draft. F.C.M. and S.L. discussed and interpreted the data. L.S. and Z.W. calculated the nucleation rates. All authors contributed to manuscript revision. All authors read and approved the final manuscript.

Notes

The authors declare no competing financial interest.

ACKNOWLEDGMENTS

S.L. and G.L. would like to acknowledge the financial support by the National Natural Science Foundation of China (Nos. 61904021, 61974012, and 21827812), the Chongqing Research Program of Basic Research and Frontier Technology (No. cstc2017jcyjBX0036), and the Chongqing Technical Innovation and Application Demonstration Program (No. cstc2018jscx-mszdX0073), Guangdong Provincial Key Laboratory of Optical Information Materials and Technology (2017B030301007), the fund of the State Key Laboratory of Solidification Processing in NWPU (Grant No. SKLSP201907). F.C.M. acknowledges funding from the UK Engineering and Physical Sciences Research Council (EPSRC) Platform Grant EP/N002423/1 and the European Research Council (ERC) under Project DYNAMIN - DLV-788968.

REFERENCES

(1) Yao, S.; Jin, B.; Liu, Z.; Shao, C.; Zhao, R.; Wang, X.; Tang, R. Biomineralization: From Material Tactics to Biological Strategy. Adv. Mater. 2017, 29, 1605903.

(2) Gorna, K.; Hund, M.; Vucak, M.; Groehn, F.; Wegner, G. Amorphous Calcium Carbonate in Form of Spherical Nanosized Particles and its Application as Fillers for Polymers. Mater. Sci. Eng., A 2008, 477, 217-225.

(3) Gong, T.; Shen, J.; Hu, Z.; Marquez, M.; Cheng, Z. Nucleation Rate Measurement of Colloidal Crystallization Using Microfluidic Emulsion Droplets. Langmuir 2007, 23, 2919.

(4) Sear, R. P. Quantitative studies of Crystal Nucleation at Constant Supersaturation: Experimental Data and Models. CrystEngComm 2014, 16, 6506-6522.

(5) Dickinson, E.; Kruizenga, F.-J.; Povey, M. J. W.; van der Molen, M. Crystallization in Oil-in-water Emulsions Containing Liquid and Solid Droplets. Colloids Surf., A 1993, 81, 273-279.

(6) Kashchiev, D.; Kaneko, N.; Sato, K. Kinetics of Crystallization in Polydisperse Emulsions. J. Colloid Interface Sci. 1998, 208, 167-177.

(7) Hindle, S.; Povey, M. J. W.; Smith, K. Kinetics of Crystallization in N-hexadecane and Cocoa Butter Oil-in-water Emulsions Accounting for Droplet Collision-mediated Nucleation. J. Colloid Interface Sci. 2000, 232, 370-380.

(8) Pham, N.; Radajewski, D.; Round, A.; Brennich, M.; Pernot, P.; Biscans, B.; Bonnete, F.; Teychene, S. Coupling High Throughput Microfluidics and Small-Angle X-ray Scattering to Study Protein Crystallization from Solution. Anal. Chem. 2017, 89, 2282-2287.

(9) Levenstein, M. A.; Anduix-Canto, C.; Kim, Y.-Y.; Holden, M. A.; Gonzalez Nin˜o, C.; Green, D. C.; Foster, S. E.; Kulak, A. N.; Govada, L.; Chayen, N. E.; Day, S. J.; Tang, C. C.; Weinhausen, B.; Burghammer, M.; Kapur, N.; Meldrum, F. C. Droplet Microfluidics XRD Identifies Effective Nucleating Agents for Calcium Carbonate. Adv. Funct. Mater. 2019, 29, 1808172.

(10) Dombrowski, R. D.; Litster, J. D.; Wagner, N. J.; He, Y. Crystallization of Alpha-lactose Monohydrate in a Drop-based Microfluidic Crystallizer. Chem. Eng. Sci. 2007, 62, 4802-4810.

(11) Laval, P.; Salmon, J. B.; Joanicot, M. A Microfluidic Device for Investigating Crystal Nucleation Kinetics. J. Cryst. Growth 2007, 303, 622-628.

(12) Spiegel, B.; Kafer, A.; Kind, M. Crystallization Behavior and¨Nucleation Kinetics of Organic Melt Droplets in a Microfluidic Device. Cryst. Growth Des. 2018, 18, 3307-3316.

(13) Li, S.; Zeng, M.; Gaule, T.; Mcpherson, M. J.; Meldrum, F. C. Passive Picoinjection Enables Controlled Crystallization in a Droplet Microfluidic Device. Small 2017, 13, 1702154.

(14) Cavanaugh, J.; Whittaker, M.; Joester, D. Crystallization Kinetics of Amorphous Calcium Carbonate in Confinement. Chem. Sci. 2019, 10, 5039-5043.

(15) Fatemi, N.; Devos, C.; Cordt, G. D.; Gerven, T. V.; Kuhn, S. Effect of Sodium Dodecyl Sulfate on the Continuous Crystallization in Microfluidic Devices Using Microbubbles. Chem. Eng. Technol. 2019, 42, 2105-2112.

(16) Zhang, S.; Gerard, C. J. J.; Ikni, A.; Ferry, G.; Vuillard, L. M.; Boutin, J. A.; Ferte, N.; Grossier, R.; Candoni, N.; Veesler, S. Microfluidic platform for optimization of crystallization conditions. J. Cryst. Growth 2017, 472, 18-28.

(17) Gerard, C. J. J.; Ferry, G.; Vuillard, L. M.; Boutin, J. A.; Ferte, N.; Grossier, R.; Candoni, N.; Veesler, S. A chemical library to screen protein and protein-ligand crystallization using a versatile microfluidic platform. Cryst. Growth Des. 2018, 18, 5130-5137.

(18) Zhu, Y.; Zhu, L.-N.; Guo, R.; Cui, H.-J.; Ye, S.; Fang, Q. Nanoliter-Scale Protein Crystallization and Screening with a Microfluidic Droplet Robot. Sci. Rep. 2015, 4, 5046.

(19) Heymann, M.; Opthalage, A.; Wierman, J. L.; Akella, S.; Szebenyi, D. M. E.; Gruner, S. M.; Fraden, S. Room-temperature serial crystallography using a kinetically optimized microfluidic device for protein crystallization and on-chip X-ray diffraction. IUCrJ 2014, 1, 349-360.

(20) Shin, Y. S.; Cho, K.; Lim, S. H.; Chung, S.; Park, S.-J.; Chung, C.; Han, D.-C.; Chang, J. K. PDMS-based micro PCR chip with Parylene coating. J. Micromech. Microeng. 2003, 13, 768-774.

(21) Teychene, S.; Biscans, B. Crystal nucleation in a droplet based´ microfluidic crystallizer. Chem. Eng. Sci. 2012, 77, 242-248.

(22) Zheng, B.; Tice, J. D.; Roach, L. S.; Ismagilov, R. F. A dropletbased, composite pdms/glass capillary microfluidic system for evaluating protein crystallization conditions by microbatch and vapor-diffusion methods with on-chip x-ray diffraction. Angew. Chem., Int. Ed. 2004, 43, 2508.

(23) Li, L.; Mustafi, D.; Fu, Q.; Tereshko, V.; Chen, D. L.; Tice, J. D.; Ismagilov, R. F. screening and optimization validated with crystallization of membrane proteins. Proc. Natl. Acad. Sci. U. S. A. 2006, 103, 19243.

(24) Fu, Y.; Zhou, H.; Jia, C.; Jing, F.; Jin, Q.; Zhao, J.; Li, G. A Microfluidic Chip Based on Surfactant-doped Polydimethylsiloxane (PDMS) in a Sandwich Configuration for Low-cost and Robust Digital PCR. Sens. Actuators, B 2017, 245, 414-422.

(25) Ning, Y.; Cui, X.; Yang, C.; Jing, F.; Bian, X.; Yi, L.; Li, G. A Self-digitization Chip Integrated with Hydration Layer for Low-cost and Robust Digital PCR. Anal. Chim. Acta 2019, 1055, 65-73.

(26) Selzer, D.; Frank, C.; Kind, M. On the Effect of the Continuous Phase on Primary Crystal Nucleation of Aqueous KNO3 Solution Droplets. J. Cryst. Growth 2019, 517, 39-47.

(27) Monahan, J.; Gewirth, A. A.; Nuzzo, R. G. A method for filling complex polymeric microfluidic devices and arrays. Anal. Chem. 2001, 73, 3193-3197.

(28) Pound, G. M.; LaMer, V. K. Kinetics of crystalline nucleus formation in supercooled liquid tin. J. Am. Chem. Soc. 1952, 74, 2323-2332.

(29) Laval, P.; Crombez, A.; Salmon, J. B. Microfluidic Droplet Method for Nucleation Kinetics Measurements. Langmuir 2009, 25, 1836-1841.

(30) Teychene, S.; Biscans, B. Microfluidic Device for the´ Crystallization of Organic Molecules in Organic Solvents. Cryst. Growth Des. 2011, 11, 4810-4818.

(31) Herbert, R. J.; Murray, B. J.; Whale, T. F.; Dobbie, S. J.; Atkinson, J. D. Representing time-dependent freezing behaviour in immersion mode ice nucleation. Atmos. Chem. Phys. Discuss. 2014, 14, 1399-1442.

(32) Diao, Y.; Helgeson, M. E.; Siam, Z. A.; Doyle, P. S.; Myerson, A. S.; Hatton, T. A.; Trout, B. L. Nucleation under Soft Confinement: Role of Polymer-solute Interactions. Cryst. Growth Des. 2012, 12, 508-517.

(33) Politi, Y.; Batchelor, D. R.; Zaslansky, P.; Chmelka, B. F.; Weaver, J. C.; Sagi, I.; Weiner, S.; Addadi, L. Role of Magnesium Ion in the Stabilization of Biogenic Amorphous Calcium Carbonate: A Structure-Function Investigation. Chem. Mater. 2010, 22, 161-166.

(34) Kitamura, M. Crystallization and Transformation Mechanism of Calcium Carbonate Polymorphs and the Effect of Magnesium Ion. J. Colloid Interface Sci. 2001, 236, 318-327.

(35) Davis, K. J.; Dove, P. M. The Role of Mg2+ as an Impurity in Calcite Growth. Science 2000, 290, 1134-1137.

(36) Zhang, Z.; Xie, Y. D.; Xu, X. R.; Pan, H. H.; Tang, R. K. Transformation of Amorphous Calcium Carbonate into Aragonite. J. Cryst. Growth 2012, 343, 62-67.

(37) Ihli, J.; Kim, Y. Y.; Noel, E. H.; Meldrum, F. C. The Effect of Additives on Amorphous Calcium Carbonate (ACC): Janus Behavior in Solution and the Solid State. Adv. Funct. Mater. 2013, 23, 1575- 1585.

(38) Kontoyannis, C. G.; Vagenas, N. V. Calcium Carbonate Phase Analysis Using XRD and FT-Raman Spectroscopy. Analyst 2000, 125, 251-255.

(39) Stephens, C. J.; Kim, Y. Y.; Evans, S. D.; Meldrum, F. C.; Christenson, H. K. Early stages of crystallization of calcium carbonate revealed in picoliter droplets. J. Am. Chem. Soc. 2011, 133, 5210- 5213.

(40) Li, S.; Ihli, J.; Marchant, W. J.; Zeng, M.; Chen, L.; Wehbe, K.; Cinque, G.; Cespedes, O.; Kapur, N.; Meldrum, F. C. Synchrotron FTIR Mapping of Mineralization in A Microfluidic Device. Lab Chip 2017, 17, 1616-1624.

(41) Zeng, M.; Kim, Y. Y.; Anduix-Canto, C.; Frontera, C.; Laundy, D.; Kapur, N.; Christenson, H. K.; Meldrum, F. C. Confinement Generates Single-crystal Aragonite Rods at Room Temperature. Proc. Natl. Acad. Sci. U. S. A. 2018, 115, 7670-7675.

(42) Leng, J.; Salmon, J. B. Microfluidic Crystallization. Lab Chip 2009, 9, 24-34.

(43) Shin, Y. S.; Cho, K.; Lim, S. H.; Chung, S.; Park, S.-J.; Chung, C.; Han, D.-C.; Chang, J. K. PDMS-based Micro PCR Chip with Parylene Coating. J. Micromech. Microeng. 2003, 13, 768-774.

(44) Zhu, Q.; Qiu, L.; Yu, B.; Xu, Y.; Gao, Y.; Pan, T.; Tian, Q.; Song, Q.; Jin, W.; Jin, Q.; Mu, Y. Digital PCR on an Integrated Selfpriming Compartmentalization Chip. Lab Chip 2014, 14, 1176-1185.

(45) Ildefonso, M.; Candoni, N.; Veesler, S. Heterogeneous Nucleation in Droplet-based Nucleation Measurements. Cryst. Growth Des. 2013, 13, 2107-2110.

(46) Wang, Y. W.; Kim, Y. Y.; Stephens, C. J.; Meldrum, F. C.; Christenson, H. K. In Situ Study of the Precipitation and Crystallization of Amorphous Calcium Carbonate (ACC). Cryst. Growth Des. 2012, 12, 1212-1217.

(47) Loste, E.; Wilson, R. M.; Seshadri, R.; Meldrum, F. C. The Role of Magnesium in Stabilising Amorphous Calcium Carbonate and Controlling Calcite Morphologies. J. Cryst. Growth 2003, 254, 206- 218.

(48) Kulak, A. N.; Iddon, P.; Li, Y. T.; Armes, S. P.; Colfen, H.; Paris, O.; Wilson, R. M.; Meldrum, F. C. Continuous Structural Evolution of Calcium Carbonate Particles: A Unifying Model of Copolymer-Mediated Crystallization. J. Am. Chem. Soc. 2007, 129, 3729-3736.

(49) De Yoreo, J. J.; Gilbert, P. U. P. A.; Sommerdijk, N. A. J. M.; Penn, R. L.; Whitelam, S.; Joester, D.; Zhang, H. Z.; Rimer, J. D.; Navrotsky, A.; Banfield, J. F.; Wallace, A. F.; Michel, F. M.; Meldrum, F. C.; Colfen, H.; Dove, P. M. Crystallization by particle attachment in synthetic, biogenic, and geologic environments. Science 2015, 349, aaa6760.

(50) Selzer, D.; Tüllmann, N.; Kiselev, A.; Leisner, T.; Kind, M. Investigation of Crystal Nucleation of Highly Supersaturated Aqueous KNO3 Solution from Single Levitated Droplet Experiments. Cryst. Growth Des. 2018, 18, 4896-4905.